SOILS AND FOUNDATIONS Vol. 45, No. 5, 103-113, Oct. 2005
Japanese Geotechnical Society

LIQUEFACTION PROPERTIES OF TOYOURA SAND IN CYCLIC TORTIONAL SHEAR TESTS UNDER LOW CONFINING STRESS

JUNICHI KOSEKI[i], TATSUYA YOSHIDA[ii] and TAKESHI SATO[iii]

ABSTRACT

A series of undrained cyclic torsional shear tests was conducted to investigate liquefaction properties of Toyoura sand under low confining stress. Hollow-cylindrical specimens were prepared by air pluviation at a relative density of about 55%. After being saturated, they were anisotropically consolidated to an effective vertical stress of 9.8, 29.4 and 98.1 kPa, while keeping the effective horizontal stress to be half of the vertical one. They were subjected to undrained cyclic torsional shear without allowing any vertical displacement of the top cap. The amplitude of the cyclic shear stress was kept constant with correction for the effects of membrane force on the measured values. The liquefaction resistance was found to increase with the decrease in the confining stress, while correction for the effects of membrane penetration did not significantly affect this tendency. Analyses of the test results revealed that the liquefaction properties were affected by the mobilization of shear resistance under extremely low effective stress states and the stress level-dependency of shear modulus that was normalized by the confining stress. Finally, by introducing a concept of apparent increase in the effective mean principal stress, a simplified procedure to estimate the liquefaction resistance under low confining stresses was proposed.

Key words: confining stress, liquefaction, membrane force, membrane penetration, sand, torsional shear (**IGC**: D6)

INTRODUCTION

In small-scale model tests conducted under normal gravity, the confining stress in the model ground is generally low. Although soil properties are known to be affected by the confining stress levels, a limited number of studies have been conducted on the effects of the confining stress on the liquefaction properties of sandy soils, due mainly to technical difficulties in controlling and measuring low stresses. Among them, based on results from undrained cyclic triaxial tests, it has been pointed out by Mochizuki and Fukushima (1993), Kanatani et al. (1994) and Amaya et al. (1997) that the liquefaction resistance of Toyoura sand increases with the decrease in the confining stress levels.

Because the behavior of level ground which is subjected to horizontal earthquake motions can be better simulated by cyclic torsional shear tests, Koseki et al. (2001) conducted a series of undrained cyclic torsional shear tests on two kinds of sands. The test results were consistent with those obtained by the undrained cyclic triaxial tests as mentioned above. However, in this series of tests, the specimen was isotropically consolidated and subjected to undrained cyclic torsional shear while maintaining the total vertical and horizontal stresses constant. There still exists, therefore, a discrepancy in the initial stress states and their changes during liquefaction, between the above series of cyclic torsional shear tests on the isotropically consolidated specimen and the relevant model tests on level ground that is one-dimensionally consolidated under anisotropic stress states.

In view of the above, in order to investigate the effects of low initial confining stress levels on the liquefaction properties of anisotropically consolidated Toyoura sand, a series of undrained cyclic torsional shear tests on hollow cylindrical specimens was conducted in the present study. In order to simulate as much as possible the simple shear condition that the level ground undergoes during horizontal excitations, the vertical displacement of the top cap was not allowed during the process of undrained cyclic torsional shear. In the whole course of the tests, due attentions were paid to control the specified stress states accurately, referring to the procedures employed by Tatsuoka et al. (1986a). As far as the authors have investigated in the literature, there exists no previous study on liquefaction properties of anisotropically consolidated sand under low confining stress.

APPARATUS

The test apparatus employed in the present study is schematically shown in Fig. 1. Major modifications with

[i] Professor, Institute of Industrial Science, The University of Tokyo, Japan (koseki@iis.u-tokyo.ac.jp).
[ii] Engineer, East Japan Railway, Japan.
[iii] Research Associate, IIS, The Univ. of Tokyo, Japan.
The manuscript for this paper was received for review on March 1, 2005; approved on July 20, 2005.
Written discussions on this paper should be submitted before May 1, 2006 to the Japanese Geotechnical Society, 4-38-2, Sengoku, Bunkyo-ku, Tokyo 112-0011, Japan. Upon request the closing date may be extended one month.

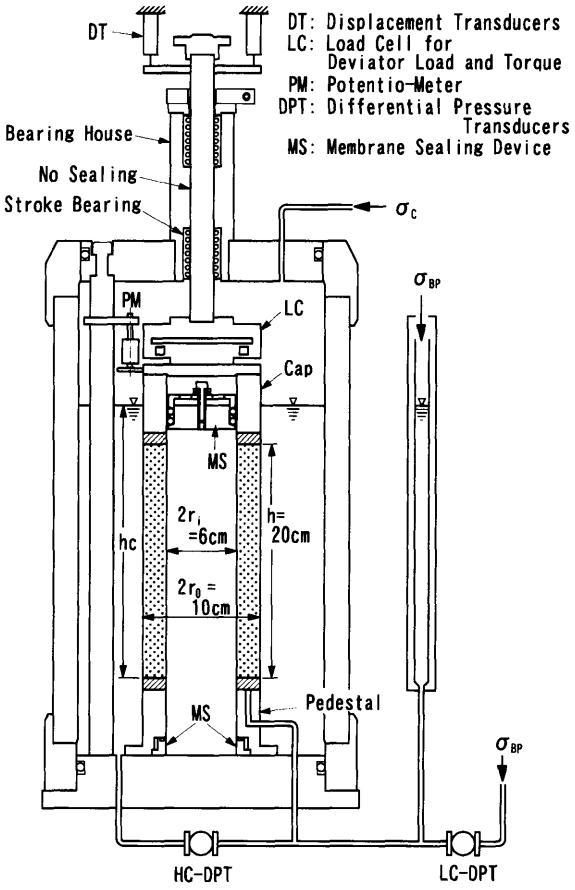

Fig. 1. Torsional shear testing apparatus (modified from Tatsuoka et al., 1986b)

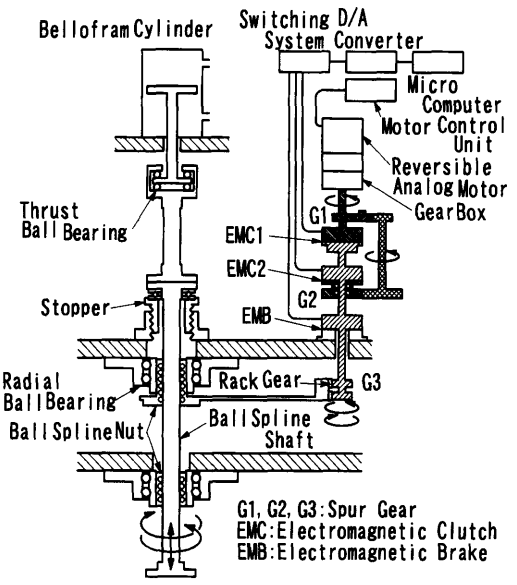

Fig. 2. Torque loading device

respect to torque loading system were made by Ampadu and Tatsuoka (1993a) from the one used by Tatsuoka et al. (1986b) and Pradhan et al. (1988), and a minor modification with adding an electro-magnetic brake for the loading system was made by the authors.

A hollow cylindrical specimen with an outer diameter of 10 cm, inner diameter of 6 cm and a height of 20 cm was set in a pressure cell and was loaded in the torsional and vertical directions independently. The vertical load was applied with a pneumatic cylinder on the specimens consolidated to an initial effective vertical stress σ'_{vo} of 98.1 kPa, while it was applied with a dead weight on the specimens consolidated to σ'_{vo} of 9.8 and 29.4 kPa. In the latter tests, to control the effective horizontal stress accurately, the difference in the water heads in two burettes which were connected to the pressure cell and the specimen was carefully adjusted to the specified values, while applying the same amount of pneumatic pressure on these burettes.

The torque was applied with an AC motor. It is connected to the loading shaft through a series of reduction-gears, two sets of electro-magnetic clutch and one electro-magnetic brake, as shown in Fig. 2. This device is a displacement-controlled type from a mechanical point of view, whereas cyclic shear tests by keeping the specified shear stress amplitude τ_d could be conducted by using a computer which monitors the outputs from a load cell and controls the device accordingly. The A/D and D/A boards of the computer had a resolution of 16 and 12 bit, respectively.

The load cell, which is capable of measuring deviator load L_c and torque T_c with negligible coupling effect between each other (refer to Tatsuoka et al., 1986b for the details), was set inside the pressure cell in order to eliminate the effects of friction between the loading shaft and the bearing house. The effective vertical stress σ'_v and the shear stress τ applied on a horizontal plane at the mid-height of the specimen were obtained as follows;

$$\sigma'_v = \sigma'_h + L_c/A_s - \gamma_w(h_c - h)A_c/A_s + \gamma'(h/2) \quad (1)$$

$$\tau = 3T_c/\{2\pi(r_o^3 - r_i^3)\} - \tau_m \quad (2)$$

$$\tau_m = t_m E_m (r_o^3 + r_i^3)\theta/\{(r_o^3 - r_i^3)h\} \quad (3)$$

where σ'_h is effective horizontal stress measured with a high-capacity differential pressure transducer (HC-DPT in Fig. 1); θ is rotational angle of the top cap measured with a potentio-meter (PM in Fig. 1); A_s and A_c are the cross-sectional areas of the specimen and the top cap, respectively; h is the height of the specimen; h_c is the relative height of the cell water level measured from the bottom of the specimen (refer to Fig. 1); r_o and r_i are outer and inner radii of the specimen; γ_w is unit weight of water; γ' is submerged unit weight of the specimen; τ_m is the apparent shear stress that is mobilized by the forces in outer and inner membranes due to torsional deformations; and t_m and E_m are thickness (=0.3 mm) and Young's modulus (=1492 kPa), respectively, of the membrane. Note that correction for the effects of membrane force on the σ'_v values was not made in the present study, since the vertical strain of the specimen accumulated during the undrained cyclic torsional shearing was maintained to be zero, by using a mechanical locking device for the vertical displacement of the top cap.

Since the outer and the inner cell pressures were kept

Table 1. Test conditions

Material and relative density		Toyoura sand (D_r = 52–56%)		
Initial effective stresses after consolidation	Horizontal	σ'_{ho} = 4.9 kPa	σ'_{ho} = 14.7 kPa	σ'_{ho} = 49.0 kPa
	Vertical	σ'_{vo} = 9.8 kPa	σ'_{vo} = 29.4 kPa	σ'_{vo} = 98.1 kPa
	Mean	p'_0 = 6.5 kPa	p'_0 = 19.6 kPa	p'_0 = 65.4 kPa
Undrained cyclic torsional shear		Constant amplitude of shear stress τ_d with correction for effects of membrane force, while not allowing vertical displacement of top cap		

equal to each other throughout the tests, the effective horizontal stress σ'_h was the same in both the radial and circumferential directions. In all the tests, the initial effective horizontal stress σ'_{ho} at the end of anisotropic consolidation was set equal to the half of σ'_{vo}. In the tests conducted under σ'_{ho} of 49.0 kPa, a pneumatic regulator that is capable of controlling a pressure between 2 to 1029 kPa was used to control the cell pressure and the back pressure. On the other hand, in the tests conducted under σ'_{ho} of 4.9 or 14.7 kPa, another regulator that is capable of controlling a pressure between 0 to 686 kPa was used. The measurable range of the HC-DPT was also adjusted accordingly.

The vertical strain ε_v during the anisotropic consolidation was obtained from the vertical displacement of the loading shaft that was measured with a displacement transducer (DT in Fig. 1). The shear strain γ mobilized on a horizontal plane at the middle radius of $r=(r_o+r_i)/2$ was obtained from the rotational angle θ of the top cap that was measured with the potentio-meter as;

$$\gamma=\theta(r_o+r_i)/2h \tag{4}$$

The volume of water ΔV_w that was expelled from the specimen during its consolidation process was measured with a low-capacity differential pressure transducer (LC-DPT in Fig. 1). Based on this measurement, while neglecting the effects of membrane penetration and surface tension of water in the burette on measured values of ΔV_w, the change in the cross-sectional area A_s of the specimen during the consolidation process was computed.

TEST PROCEDURES

Hollow cylindrical specimens of Toyoura sand (G_s = 2.635, e_{max} = 0.966, e_{min} = 0.600, D_{50} = 0.18 mm with no fines content under 75 μm) were prepared by pluviating air-dried sand particles through air.

As listed in Table 1, three conditions of anisotropic consolidation were employed in the present study, where the initial effective vertical stress σ'_{vo} at the end of consolidation was set at 9.8, 29.4, and 98.0 kPa while keeping the initial effective horizontal stress σ'_{ho} to be half of the vertical one.

The specimens to be consolidated to σ'_{ho} = 49.0 kPa were saturated at an isotropic effective stress state of 29.4 kPa with the double vacuuming method using partial vacuum as both the pore water pressure and the cell pressure (Ampadu and Tatsuoka, 1993b). On the other hand, the specimens to be consolidated to σ'_{ho} = 4.9 and 14.7 kPa were saturated at an isotropic effective stress state of 3.9 and 9.8 kPa, respectively, with pouring carbon dioxide through the void among the sand particles and then pouring de-aired water. After confirming that the B value of the specimens is not smaller than 0.96, the stress state was changed to an anisotropic by increasing the effective vertical stress σ'_v, while keeping σ'_h constant. Subsequently, the specimens were anisotropically consolidated by increasing σ'_v and σ'_h to the specified values, while maintaining the ratio σ'_h/σ'_v to be 0.5.

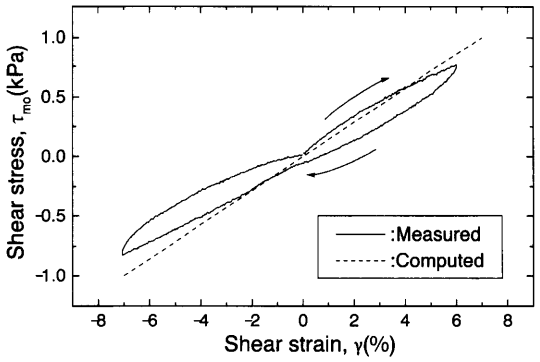

Fig. 3. Apparent stress and strain relationships in torsional shear test on outer membrane without specimen

The initial relative density, D_r, of each specimen was obtained from the specimen dimensions measured under a state immediately before the saturation process and from its dry weight measured after the tests. It should be noted that, the change in the relative density measured during the anisotropic consolidation process from σ'_h = 29.4 kPa to σ'_h = 49.0 kPa, which was evaluated from the amount of water expelled from the specimen, was relatively small, as compared to the variation in the values D_r among different specimens. Therefore, possible effects of the difference in the confining stress levels at which the initial relative density was measured (i.e., at 3.9, 9.8 and 29.4 kPa) on the test result was not considered in the present study.

From the specified anisotropic stress states, the torsional load was cyclically changed under undrained condition with maintaining the specified single amplitude of the shear stress τ_d that was corrected for the effects of membrane force, while not allowing the vertical displacement of the top cap. The shear strain rate was about

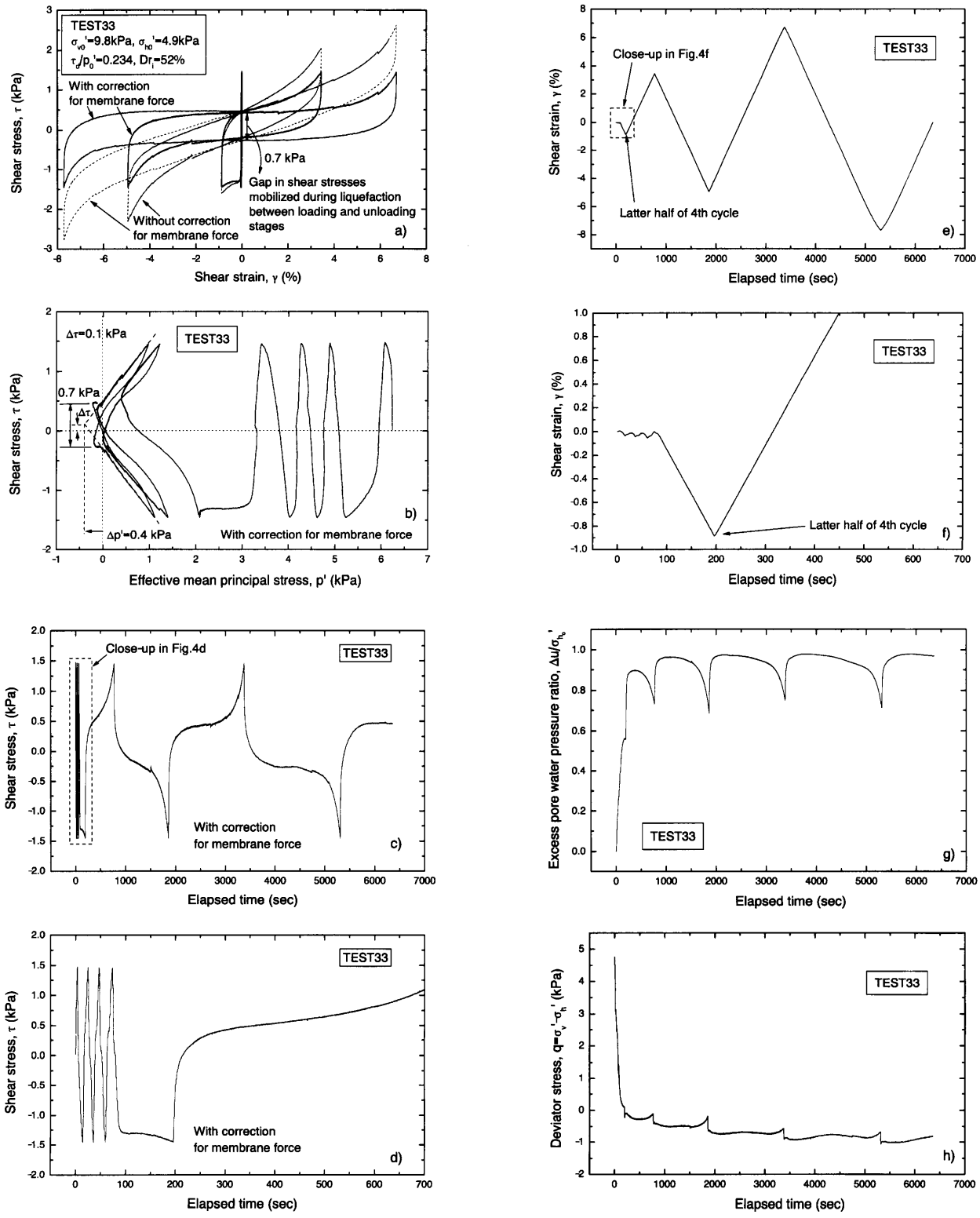

Fig. 4. Results from test 33 ($p_0' = 6.5$ kPa, $\tau_d / p_0' = 0.234$, $D_{r_i} = 52\%$)

0.5%/min. The cyclic loading was terminated when the double amplitude of the shear strain γ_{DA} exceeded about 10%.

TEST RESULTS AND DISCUSSIONS

Validation of Correction of Torsional Shear Stress for Membrane Force

In order to confirm Eq. (3) in correcting for the effects of membrane force on the measured shear stress, a special

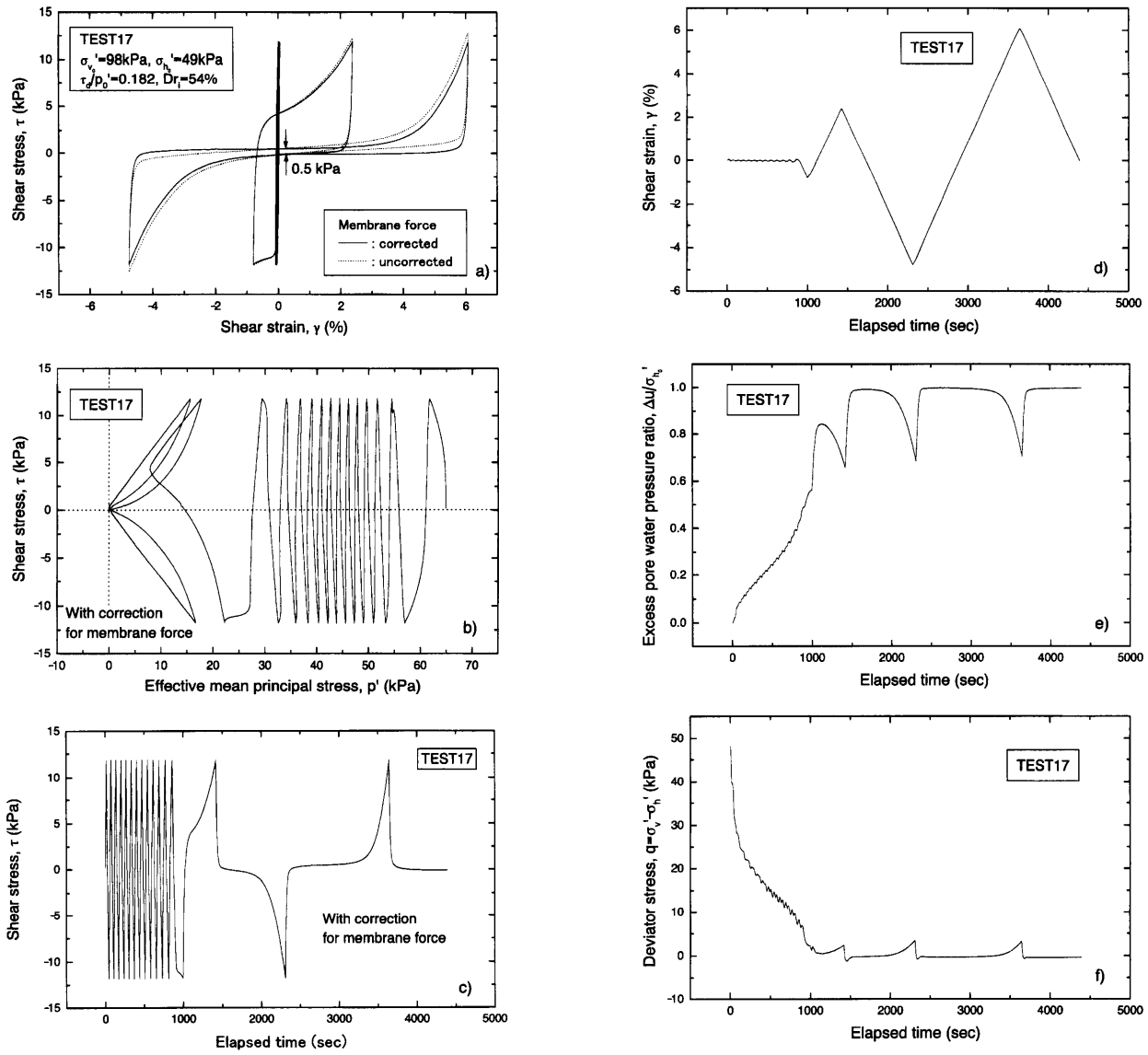

Fig. 5. Results from test 17 ($p_0' = 65.4$ kPa, $\tau_d / p_0' = 0.182$, $D_r = 54\%$)

test was performed. In this test, only the outer membrane was set to the top cap and the pedestal without the soil specimen or the inner membrane, and the top cap was cyclically rotated while fixing its vertical displacement. During this cyclic rotation, the air in the inner space of the membrane was sealed, in order to simulate as much as possible the constant volume condition during the undrained cyclic torsional shear process in the actual tests. As shown in Fig. 3, the measured relationship between the apparent shear stress τ_{mo} due to torsional deformation of outer membrane and the shear strain γ was consistent with the computed one. τ_{mo} was evaluated by using Eq. (5) that was obtained from Eq. (3) considering the absence of inner membrane for this special test.

$$\tau_{mo} = t_m E_m r_o^3 \theta / \{(r_o^3 - r_i^3)h\} \quad (5)$$

Typical Behavior during Undrained Cyclic Loading

Observed behavior in test 33 where the specimen was consolidated to $p_0' = 6.5$ kPa and subjected to undrained cyclic loading with a cyclic stress ratio of $\tau_d / p_0' = 0.234$ is shown in Figs. 4(a) through 4(h). Note that p_0' is the initial effective mean principal stress ($= (\sigma_{vo}' + 2\sigma_{ho}')/3$) and is used for defining the cyclic stress ratio herein.

In Fig. 4(a), stress-strain relationships based on shear stresses with/without correction for the membrane force are compared. It is obvious that correction for the membrane force is indispensable in conducting torsional shear tests under low confining stresses, similarly to the cases with triaxial tests and plane strain compression tests as pointed out by Fukushima and Tatsuoka (1984) and Tatsuoka et al. (1986c). On the other hand, under relatively high confining stresses, the effect of correction for the membrane force on the shear stress is less significant as typically shown in Fig. 5(a) for test 17 that was conducted at $p_0' = 65.4$ kPa with $\tau_d / p_0' = 0.182$.

In Fig. 4(b), the effective stress path for test 33 is shown in terms of the shear stress τ and the current effective

mean principal stress p' $(=(\sigma'_v+2\sigma'_h)/3)$. It can be seen that the stress path did not pass through the origin (i.e., $\tau=p'=0$). Similar behavior was also observed in other tests conducted at $p'_0=6.5$ kPa. Discussion on this behavior will be made later.

Figures 4(c) through 4(h) show individual data plotted versus the elapsed time t. Since the torsional load was applied under constant shear strain rate as shown in Figs. 4(e) and 4(f), the period of each cyclic loading was shorter in the first few cycles. Subsequently, with the increase in the shear strain amplitude, the period of each cyclic loading became longer. It can be seen from Figs. 4(c) and 4(d) that the constant amplitude of cyclic shear stress τ_d that was corrected for the effects of membrane force could be controlled successfully during the whole stages of cyclic loading under low confining stress. By using the same apparatus, accurate control of the cyclic shear stress under relatively high confining stress could be also made (Figs. 5(c) and 5(d)).

Although the shear strain amplitude in the first few cycles was on the order of 0.01% (Fig. 4(f)), the excess pore water pressure Δu accumulated gradually as shown in Fig. 4(g). It was accompanied by a decrease in the deviator stress q $(=\sigma'_v-\sigma'_h)$ as shown in Fig. 4(h). In this test, during the unloading stage in the fifth cycle around $t=1000$ sec, the value of Δu became almost equal to the initial confining stress σ'_{ho}, suggesting an occurrence of initial liquefaction. After the occurrence of initial liquefaction, the change in the q value became less significant, except for its temporary recovery that was caused by mobilization of positive dilatancy with the application of torsional shear stresses in both directions. Similar response was observed with the tests conducted under higher confining stress levels (Figs. 5(e) and 5(f)).

It should be noted that, as can be seen from Fig. 5(f), the q value after the occurrence of initial liquefaction should have been stabilized at zero. Strictly speaking, however, it was not always the case with the tests conducted under low confining stress as typically shown in Fig. 4(h). The latter peculiar behavior is possibly affected by long-term shift in the output of load cell and/or distortion of load cell due to misalignment of the specimen with respect to the loading shaft. Further modification is required to reduce these possible errors.

Liquefaction Resistance Curves and Their Correction for Effects of Membrane Penetration

Relationship between the cyclic stress ratio τ_d/p'_0 and the number of cycles N_c, to induce a double amplitude shear strain γ_{DA} of 7.5% is shown in Fig. 6. The liquefaction resistance increased with the decrease in the confining stress.

In this study, the vertical displacement of the top cap was not allowed during the process of cyclic torsional shear, while keeping the undrained condition at the same time. Therefore, the effects of membrane penetration (referred to as MP hereafter) on the present test results would have been smaller than those on tests conducted without such axial strain constraint. However, in order to

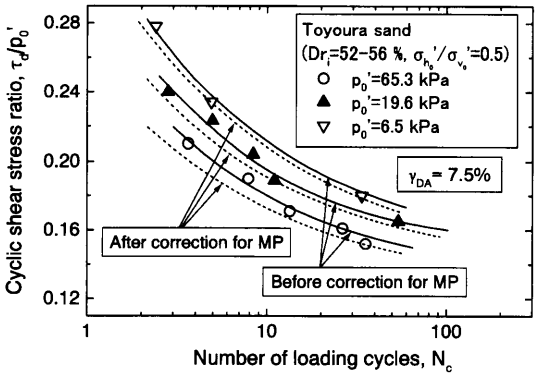

Fig. 6. Liquefaction resistance curves

correct for the effects of MP to maximum possible extents, it was hereafter attempted to modify the liquefaction resistance curves based on the results from previous relevant studies. They were obtained by the following procedures:

a) Increment of volumetric strain due to decrease in the effective mean principal stress p' was evaluated experimentally on Toyoura sand at $D_r=56\%$ by Shahnazari (2001) and was formulated as:

$$d\varepsilon_{vol}=\frac{f(p')}{p'\cdot\log_e 10}\cdot dp' \tag{6}$$

$$f(p')=0.00386-(1.98046\times10^{-5})p'+(5.05301\times10^{-8})p'^2-(4.7336\times10^{-11})p'^3 \tag{7}$$

where the physical unit of p' in Eq. (7) is kPa. In the present study, volumetric strain $\Delta\varepsilon_{vol}$ due to liquefaction was estimated by integrating the above formulation as:

$$\Delta\varepsilon_{vol}=\int_{p'_0}^{p'_f}d\varepsilon_{vol}=\int_{p'_0}^{p'_f}\frac{f(p')}{p'\cdot\log_e 10}\cdot dp' \tag{8}$$

where p'_f is the effective mean principal stress at liquefaction. Since p'_f had to be positive in the above formulation, it was set equal to 1 kPa as a first approximation.

b) The apparent volumetric strain $\Delta\varepsilon_{vol,MP}$ due to the effects of MP during liquefaction process was obtained as:

$$\Delta\varepsilon_{vol,MP}=\frac{m_p\cdot2\pi(r_o-r_i)h}{\pi(r_o^2-r_i^2)h} \tag{9}$$

where m_p is the apparent volume change due to MP per unit surface area of the membrane. As shown in Fig. 7, the value of m_p was estimated by extrapolating the experimental evaluation that was made by Shahnazari (2001). With the decrease in the initial effective horizontal stress, as can be seen from the figure, the value of m_p is decreased although the rate of its change is increased.

c) Based on the above estimations, the system compliance ratio C_R due to MP was evaluated as:

$$C_R\equiv\frac{K_S}{K_{C,MP}}=\frac{\Delta p'/\Delta\varepsilon_{vol}}{\Delta p'/\Delta\varepsilon_{vol,MP}}=\frac{\Delta\varepsilon_{vol,MP}}{\Delta\varepsilon_{vol}} \tag{10}$$

where K_S is the bulk modulus of the tested soil, and $K_{C,MP}$ is the apparent bulk modulus due to MP. Subsequently,

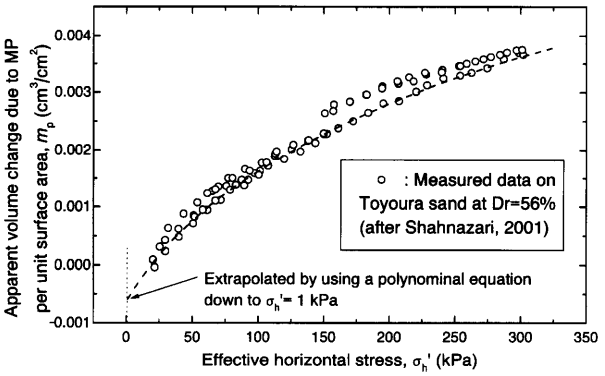

Fig. 7. Estimation of apparent volume change due to membrane penetration

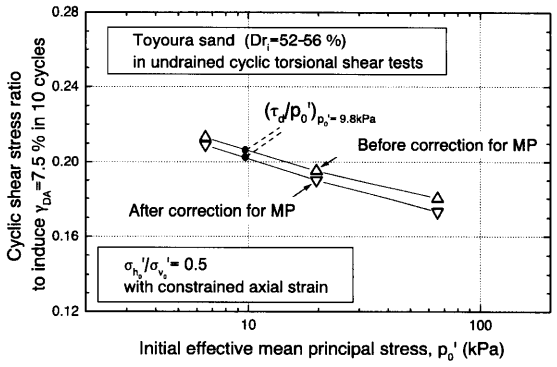

Fig. 8. Relationship between liquefaction resistance and initial effective mean principal stress

Table 2. Values of C_R and C_N

Initial effective mean principal stress, p_0'	System compliance ratio, $C_R=\Delta\varepsilon_{vol,MP}/\Delta\varepsilon_{vol}$	Cycle ratio, $C_N=N_c/N_0$
6.5 kPa	0.07	1.13
19.6 kPa	0.11	1.22
65.4 kPa	0.21	1.45

the cycle ratio $C_N=N_c/N_0$ to convert the measured number of cycles N_c into the corrected number of cycles N_0 was evaluated based on the relationships between C_R and C_N proposed by Tokimatsu and Nakamura (1987).

Table 2 summarizes the result of the above correction in terms of the values of C_R and C_N for respective confining stress levels. Based on these results, the modified liquefaction resistance curves with correction for the effects of MP are obtained as shown in Fig. 6. Since the tested sand was fine sand, the effects of MP were to limited extents, and thus the dependency of liquefaction resistance on the confining stress levels was not significantly affected by them.

Effects of Confining Stress on Liquefaction Resistance

In the present study, the value of cyclic shear stress ratio τ_d/p_0' to induce γ_{DA} of 7.5% in 10 cycles was defined as liquefaction resistance. It was evaluated based on the liquefaction resistance curves with/without correction for the effects of MP as shown in Fig. 6, and plotted in Fig. 8 versus the initial effective mean principal stress p_0' on a semi-logarithmic scale. The liquefaction resistance increased with the decrease in p_0'.

In order to compare the above effects of confining stress levels on the liquefaction resistance of Toyoura sand with those obtained in the previous studies, the liquefaction resistance at p_0' equal to 9.8 kPa was read from Fig. 8 and used as a normalizing parameter $(\tau_d/p_0')_{p_0'=9.8\,kPa}$ to compute the liquefaction resistance ratio as:

$$R_c=(\tau_d/p_0')/(\tau_d/p_0')_{p_0'=9.8\,kPa} \quad (11)$$

Similar normalization was made on the results from triaxial tests by Kanatani et al. (1994) and on those from

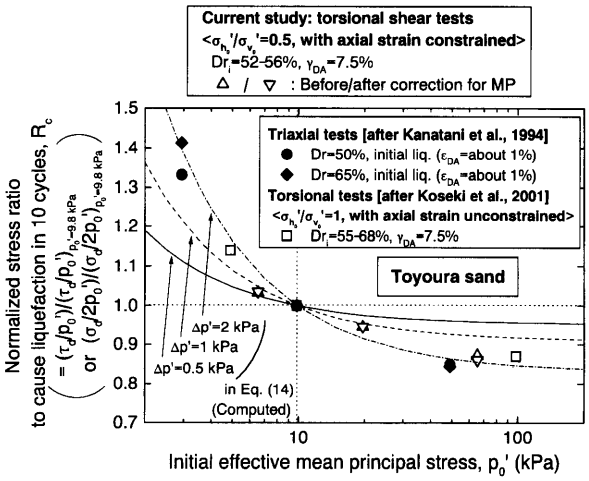

Fig. 9. Relationship between normalized liquefaction resistance and initial effective mean principal stress

torsional shear tests by Koseki et al. (2001). Both of these tests were conducted on isotropically consolidated Toyoura sand. In dealing with the triaxial test results, the following ratio was computed:

$$R_c=(\sigma_d/2\sigma_c')/(\sigma_d/2\sigma_c')_{\sigma_c'=9.8\,kPa} \quad (12)$$

where $\sigma_d/2\sigma_c'$ is the liquefaction resistance defined as the ratio between the amplitude of cyclic deviator stress σ_d and twice of the initial effective confining stress σ_c' ($=p_0'$) to cause initial liquefaction (i.e., the state of excess pore water ratio $\Delta u/\sigma_c'$ equal to unity) in 10 cycles. Note that when the state of initial liquefaction was attained in the tests by Kanatani et al. (1994) on specimens at $D_r=50\%$ and 65%, the value of the double amplitude axial strain ε_{DA} was reported to be about 1%.

Figure 9 shows the values of R_c plotted versus the initial effective mean principal stress p_0'. Under the test conditions employed in these studies (i.e., at moderately dense states with D_r in the range of 50 to 70%), the increase in the R_c values with the decrease in the p_0' values was comparable to each other among different tests. When the p_0' values decrease from 100 kPa to 10 kPa, the liquefaction resistance increases by at least 10%. On the other hand, when the p_0' values decrease further from 10

kPa, the liquefaction resistance seems to increase more rapidly.

Possible Effects of Self Weight of Specimen on Liquefaction Resistance

As mentioned before on Eq. (1), the effective stresses employed in the present study are evaluated at the mid-height of the specimen. Due to the effects of self weight of the specimen, the actual effective stress levels become larger and smaller, respectively, at the bottom and top of the specimen.

For example, by neglecting the last term in the right-hand side of Eq. (1), the effective vertical stress at the top of the specimen will be reduced by about 1 kPa from the nominal value defined at the mid-height. Similarly, the effective vertical stress at the bottom of the specimen will be increased by about 1 kPa. On the other hand, the effective horizontal stresses are the same irrespective of the location, since the pressure cell is filled with water to a height above the top of the specimen. Therefore, under the test condition with the smallest initial effective stresses after consolidation (i.e., the nominal values of the effective vertical and horizontal stresses defined at the mid-height are 9.8 kPa and 4.9 kPa, respectively), the actual values of initial effective mean principal stress p_0' will vary in the range of 6.2 to 6.9 kPa. In the present study, while referring to the sensitivity of liquefaction resistance to the nominal confining stress levels as shown in Figs. 8 and 9, possible effects of such variation in the actual effective stress levels within the specimen was assumed to be negligible.

It should be noted, however, that the state of zero effective stress during liquefaction process can not be mobilized simultaneously in all the regions of the specimen due to the above-mentioned different effects of its self weight on the vertical and horizontal stresses. Such limitation is inevitable in so-called "laboratory element tests" that are conducted under the gravitational field on soils having the specific gravity larger than that of water. Thus, this issue was regarded to be out of the scope of the present study.

Comparison of Stress-Strain Relationships and Effective Stress Paths

It can be seen from Figs. 4(a) and 5(a) that the shape of the stress-strain relationship at the liquefied states under low confining stress was different from the one obtained under higher confining stress. In particular, the histeresis loop was relatively larger in the former case. As indicated in Fig. 4(a), there was a gap of about 0.7 kPa in the shear stresses mobilized during liquefaction at the state of $\gamma=0$ between the loading (i.e., $d\tau>0$) and unloading ($d\tau<0$) stages. This amount of gap is quantitatively consistent with the one shown in Fig. 5(a). Similar amount of gap was also observed by Koseki et al. (2001) in undrained cyclic torsional shear tests without the axial strain constraint on dense Kasumigaura sand that was isotropically consolidated at $p_0'=4.9$ and 9.8 kPa.

As mentioned before, the effective stress path shown in

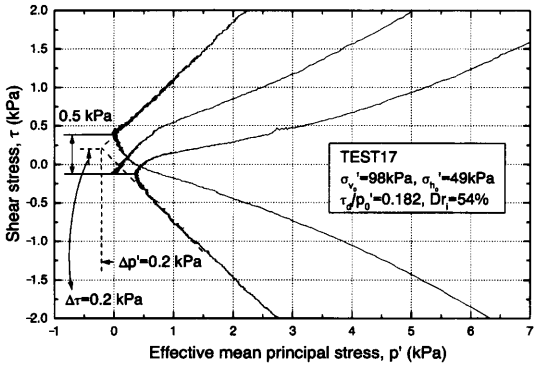

Fig. 10. Close-up around the origin of effective stress path in test 17

Fig. 4(b) did not pass through the origin ($\tau=p'=0$). As shown in Fig. 10 that is a close-up around the origin of Fig. 5(b), it was also the case with the tests conducted under higher confining stress. This behavior is possibly affected by the following two factors: a) effects of interlocking among sand particles that could be mobilized even under extremely low effective stress states, and b) errors in the measured deviator stress q as mentioned before, which would cause apparently non-zero values of p'. The latter factor b) will result into a horizontal shift of the effective stress path, while the former factor a) can explain as well the cause for the above gap in the shear stresses that were mobilized during liquefaction between the loading and unloading stages.

Based on results from a series of special direct shear tests by tilting the whole apparatus under low initial effective normal stress states in the range of 2.0 to 9.3 kPa, Kokusho et al. (2002) reported that Toyoura sand at $D_r=60\%$ has an apparent cohesion of 1.0 kPa when its failure envelope is assumed as a straight line. This may be also attributed to the effects of interlocking of sand particles. Since this value of the apparent cohesion reported by Kokusho et al. (2002) is too large to explain the above gap in the mobilized shear stresses during liquefaction in the present test results (i.e., in the range of 0.5 to 0.7 kPa for the double amplitude), further studies are required for detailed investigation on the above behavior, while improving the accuracy of measurements under extremely low effective stress states.

It should be noted that the sand behavior under extremely low effective stress states is also affected by the strain rate, exhibiting viscous properties as investigated by Towhata and Gallage (2003) among others. This behavior suggests that the above mobilization of shear resistance at extremely low effective stress states may be due not only to the interlocking effects but also to the viscous interaction between pore water and the surface of sand particles. The present tests were conducted under a relatively low strain rate of about 0.5%/min, and thus the observed amount of the gap in the mobilized shear stresses during liquefaction may have been smaller as compared to the apparent cohesion obtained by Kokusho et al. (2002) who defined the failure state at a strain rate of 6%/min (=0.1%/s).

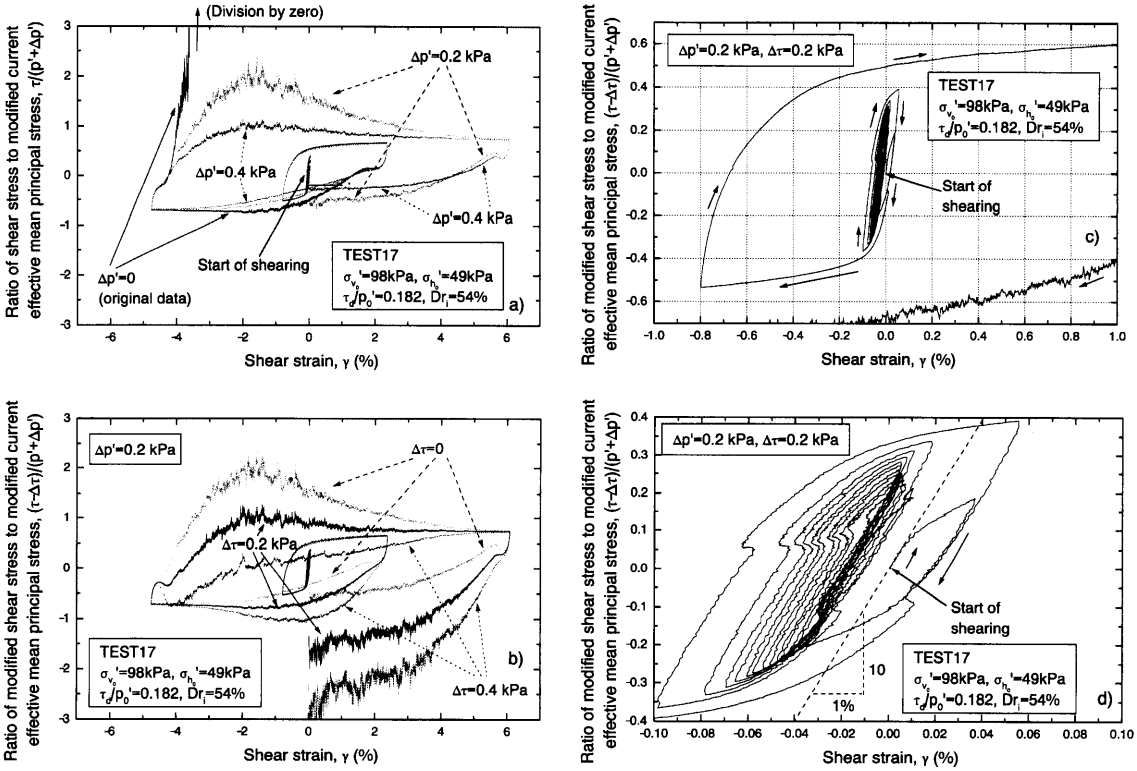

Fig. 11. Modified stress-strain relationships in test 17

Analyses of Current Shear Stress Ratio-Strain Relationships

In discussing the cyclic deformation behavior observed in this study, several attempts are made, which include introduction of apparent increase in effective mean principal stress $\Delta p'$ to correct for the mobilization of shear resistance under extremely low confining stress states.

Figure 11(a) shows the relationships between the current shear stress ratio and the shear strain γ in test 17, where the stress ratio was obtained by normalizing the shear stress τ with the current effective mean principal stress p' with/without correction for the above $\Delta p'$. Referring to Fig. 10, the amount of $\Delta p'$ was set equal to 0.2 kPa, while the condition of $\Delta p' = 0.4$ kPa was also employed for comparison. It can be seen from Fig. 11(a) that, without the correction (i.e., the case with $\Delta p' = 0$), the current shear stress ratio became unrealistically large (due to division by zero) after the specimen underwent large deformation at a γ value around -5%. On the other hand, with the correction by using $\Delta p' = 0.2$ kPa, such peculiar behavior disappeared, while strain softening behavior was observed duing the reloading path at γ values in the range of -5% to 6%. By increasing the value of $\Delta p'$ up to 0.4 kPa, such strain softening behavior disappeared as well.

It should be noted that the effective stress path shown in Fig. 10 suggests that the origin of the shear stress may have been shifted slightly, as well as the deviator stress as mentioned earlier. In Fig. 11(b), therefore, further attempts are made by introducing another correction for the shift in the shear stress $\Delta\tau$ by 0.2 kPa under a fixed value of $\Delta p'$ at 0.2 kPa. For comparison, correction with the condition of $\Delta\tau = 0.4$ kPa is also made. Consequently, the aforementioned strain softening behavior at $\Delta\tau = 0$ disappeared in both cases, while the correction by using $\Delta\tau = 0.4$ kPa resulted into too large values of the modified stress ratio in the negative side after the reversal of shearing direction.

Based on the above comparison, the correction by using $\Delta p' = 0.2$ kPa and $\Delta\tau = 0.2$ kPa is adopted herein for the results from test 17 that was conducted at $p_0' = 65.4$ kPa. Under these conditions, the close-ups of the relationships between the modified current shear stress ratio and the shear strain are shown in Figs. 11(c) and 11(d). It can be seen from Fig. 11(c) that the shear strain amplitude increased remarkably after the stress ratio exceeded about 0.4 in the negative side. Below this level of stress ratio, as shown in Fig. 11(d), the increase in the shear strain amplitude was to a limited extent.

For the results from test 33 that was conducted at $p_0' = 6.5$ kPa, correction of the shear stress ratio by using $\Delta p' = 0.4$ kPa and $\Delta\tau = 0.1$ kPa is adopted, referring to the effective stress path shown in Fig. 4(b). With this correction, the behavior at large strain levels changed significantly, as shown in Fig. 12(a). As can be seen from Figs. 12(b) and 12(c), the close-ups of the relationships between the modified current shear stress ratio and the shear strain were in general similar to those obtained in test 17 that was conducted under higher confining stress (Figs. 11(c) and 11(d)). It should be noted, however, that the amounts of normalized initial stiffness as shown by

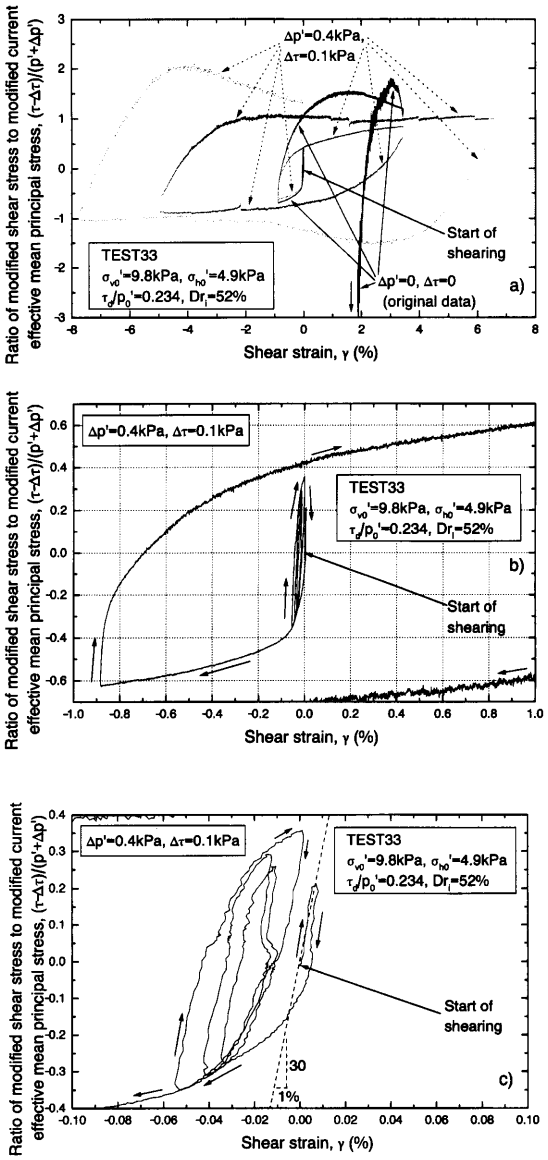

Fig. 12. Modified stress-strain relationships in test 33

dash lines in Figs. 11(d) and 12(c) were different from each other.

The above difference in the normalized initial stiffness can be explained by considering the stress state dependency of shear modulus as follows.

a) It can be seen from Fig. 11(d) that the value of the normalized initial stiffness, defined as $d\{(\tau-\Delta\tau)/(p'+\Delta p')\}/d\gamma$, in test 17 at $p_0'=65.4$ kPa is approximately 1000 ($=10/(1\%)$). By neglecting smaller terms, the shear modulus G ($=d\tau/d\gamma$) is given as 65 MPa ($=1000\times65$ kPa). This value is comparable to the range of the quasi-elastic shear modulus of Toyoura sand reported in the previous studies under similar density and confining stress levels (e.g., HongNam and Koseki, 2005, among others).

b) In the previous studies, it has also been reported that the quasi-elastic shear modulus of Toyoura sand is approximately proportional to the square root of the effective stress level. Then, the value of G in test 33 at the stress level of $p_0'=6.5$ kPa will be reduced by a factor of 3.2 ($=(65.4/6.5)^{0.5}$) as compared to the above value in test 17 at $p_0'=65.4$ kPa. Since the level of p_0' is reduced by a factor of 10 ($=65.4/6.5$) at the same time, the initial stiffness that is normalized by p_0' will increase approximately to 3000 ($=1000\times10/3.2$).

c) As shown in Fig. 12(c), the above estimation of the normalized initial stiffness in test 33 is consistent with the measured behavior.

Such stress level-dependency of normalized initial stiffness would affect the liquefaction properties as well. With the decrease in the confining stress, the normalized stiffness during cyclic loading would increase in general, and thus the amount of shear strains under the same amplitude of the cyclic shear stress ratio τ_d/p_0' would decrease. This would result into less mobilization of negative dilatancy during cyclic loading, and thus the liquefaction resistance would increase. Further investigations are required on this issue, since the experimental data obtained in the present study have a limitation in their accuracy at small strain levels, due to the errors that are involved in using external measurement of shear strain with a potentio-meter having a large capacity. For example, in the close-up figures (Figs. 11(d) and 12(c)), sudden shifts and relatively large variations of the measured shear strain were observed.

Simplified Procedure to Estimate Liquefaction Resistance under Low Confining Stresses

Herein, attempts are made to consider the effect of the apparent increase in effective mean principal stress $\Delta p'$ in estimating the liquefaction resistance under low confining stresses.

By introducing the above concept, the cyclic shear stress ratio τ_d/p_0' can be modified into $\tau_d/(p_0'+\Delta p')$. Supposing that there exists a unique liquefaction resistance in terms of this modified cyclic shear stress ratio $\{\tau_d/(p_0'+\Delta p')\}_{liq}$, the liquefaction resistance in terms of the original definion of the cyclic shear stress ratio is given as:

$$\tau_d/p_0' = \{(p_0'+\Delta p')/p_0'\} \times \{\tau_d/(p_0'+\Delta p')\}_{liq} \quad (13)$$

Then, the liquefaction resistance ratio R_c as defined by Eq. (11) can be formulated as:

$$R_c = (\tau_d/p_0')/(\tau_d/p_0')_{p_0'=9.8\,kPa} = \{(p_0'+\Delta p')/p_0'\}/\{(9.8+\Delta p')/9.8\} \quad (14)$$

Relationships between p_0' and R_c that were computed by setting the $\Delta p'$ value at 0.5, 1 and 2 kPa, respectively, in Eq. (14) are shown in Fig. 9. When compared with the experimental data, it can be seen that the assumption of $\Delta p'=0.5$ kPa was not enough to explain the dependency of liquefaction resistance on the confining stress levels. Rather, the assumption of $\Delta p'=1$ or 2 kPa could result into better simulation of the observed tendency. Although these values of $\Delta p'$ are larger than those employed in the correction of the current shear stress ratio-strain relationships as mentioned in the previous section, the extra amount in the $\Delta p'$ values might as well

account for the aforementioned effects of the stress level-dependency of shear modulus on liquefaction resistance.

Thus, in estimating liquefaction resistance $(\tau_d/p'_{low})_{liq}$ under a low confining stress at $p'_0 = p'_{low}$, the following approximate conversion may be applied to the test results obtained under a certain reference confining stress at $p'_0 = p'_{ref} (> p'_{low})$:

$$(\tau_d/p'_{low})_{liq} = (\tau_d/p'_{ref})_{liq} \times \{(p'_{low} + \Delta p'_{cor})/p'_{low}\} / \{(p'_{ref} + \Delta p'_{cor})/p'_{ref}\} \quad (15)$$

where $(\tau_d/p'_{ref})_{liq}$ is the observed liquefaction resistance, and $\Delta p'_{cor}$ is a parameter that should in principle depend on several factors such as the soil gradation, density, particle shape and crushability. In dealing with fine, clean and moderately dense sands having material properties that are similar to those of Toyoura sand tested in this study, $\Delta p'_{cor}$ can be empirically set at 1 to 2 kPa. For conservative estimation, however, assigning a smaller value of $\Delta p'_{cor}$ may be recommended.

CONCLUSIONS

The results from a series of undrained cyclic torsional shear tests on anisotropically consolidated Toyoura sand could be summarized as follows:

a) In conducting undrained cyclic torsional shear tests under low confining stresses, correction of the measured shear stress for the effects of membrane force is indispensable.

b) The liquefaction resistance increased with the decrease in the confining stress, while correction for the effects of membrane penetration did not significantly affect this tendency.

c) The liquefaction properties were affected by the mobilization of shear resistance under extremely low effective stress states and the stress level-dependency of shear modulus that is normalized by the confining stress.

d) By introducing a concept of apparent increase in the effective mean principal stress, a simplified procedure to estimate the liquefaction resistance under low confining stresses was proposed.

Further investigations are required on the physical mechanism for the above mobilization of shear resistance, while improving the accuracy of measurements under extremely low effective stress states. In performing such tests, effects of self weight of the specimen should be properly taken into account, except for the special cases that are conducted under microgravity environment (Sture et al., 2005).

Effects of the stress level-dependency of shear modulus on the liquefaction properties should be also analyzed quantitatively, based on relevant test results with improved accuracy for small strain measurements.

REFERENCES

1) Amaya, M., Sato, T., Koseki, J. and Maeshiro, N. (1997): Undrained cyclic shear characteristics of Toyoura sand under low confining stress, *Proc. 52nd Annual Conf. Jpn. Soc. Civil Engineers*, (3-A), 130–131 (in Japanese).
2) Ampadu, S. K. and Tatsuoka, F. (1993a): A hollow cylinder torsional simple shear apparatus capable of a wide range of shear strain measurement, *Geotech. Test. J.*, **16** (1), 3–17.
3) Ampadu, S. K. and Tatsuoka, F. (1993b): Effects of setting method on the behavior of clays in triaxial compression from saturation to undrained shear, *Soils and Foundations*, **33** (2), 14–34.
4) Fukushima, S. and Tatsuoka, F. (1984): Strength and deformation characteristics of saturated sand at extremely low pressures, *Soils and Foundations*, **24** (4), 30–48.
5) HongNam, N. and Koseki, J. (2005): Quasi-elastic deformation properties of Toyoura sand in cyclic triaxial and torsional loadings, *Soils and Foundations*, **45** (5), 19–38.
6) Kanatani, M., Nishi, K. and Tanaka, Y. (1994): Dynamic properties of sand at low confining pressure, *Pre-failure Deformation of Geomaterials*, (eds. by Shibuya, Mitachi and Miura), Balkema, **1**, 37–40.
7) Kokusho, T., Iwamoto, I. and Sato, T. (2002): Strength property of sand in drained monotonic loading test under low confining pressure, *Proc. 37th Jpn. Nat. Conf. Geotech. Engrg.*, 437–438 (in Japanese).
8) Koseki, J., Itakura, D., Kawakami, S. and Sato, T. (2001): Cyclic torsional shear tests on liquefaction resistance of sands under low confining stress, *Proc. 4th Int. Conf. Recent Advances in Geotechnical Earthquake Engineering and Soil Dynamics*, CD-ROM.
9) Mochizuki, Y. and Fukushima, S. (1993): Liquefaction characteristics of saturated sand at low pressure, *Proc. 28th Jpn. Natl. Conf. SMFE*, 917–918 (in Japanese).
10) Pradhan, T. B. S., Tatsuoka, F. and Horii, N. (1988): Simple shear testing on sand in a torsional shear apparatus, *Soils and Foundations*, **28** (2), 95–112.
11) Shahnazari, H. (2001): Experimental investigation on volume change and shear deformation characteristics of sand undergoing cyclic loading, *PhD Thesis*, Univ. of Tokyo.
12) Sture S., Batiste, S. Lankton, M. and Parisi, J. (2005): Cyclic behavior of sand under very low effective stresses, *Geomechanics: Testing, Modeling and Simulation, Geotechnical Special Publication*, ASCE, **143**, 187–204.
13) Tatsuoka, F., Goto, S. and Sakamoto, M. (1986a): Effect of some factors on strength and deformation characteristics of sand at low pressure, *Soils and Foundations*, **26** (1), 105–114.
14) Tatsuoka, F., Sonoda, S., Hara, K., Fukushima, S. and Pradhan, T. B. S. (1986b): Failure and deformation of sand in torsional shear, *Soils and Foundations*, **26** (4), 79–97.
15) Tatsuoka, F., Sakamoto, M., Kawamura, T. and Fukushima, S. (1986c): Strength and deformation characteristics of sand in plane strain compression at extremely low pressures, *Soils and Foundations*, **26** (1), 65–84.
16) Tokimatsu, K. and Nakamura, K. (1987): A simplified correction for membrane compliance in liquefaction tests, *Soils and Foundations*, **27** (4), 111–122.
17) Towhata, I. and Gallage, C. P. K. (2003): Rate-dependency of sand under low effective stress as observed in laboratory shear tests, *Proc. 8th US-Japan Workshop on Earthquake Resistance Design of Lifeline Facilities and Countermeasures against Liquefaction*, paper II-7, Tokyo, MCEER-03-0003, 437–448.